Volume 42 | Number 9 | 7 May 2018 | Pages 6551–7488

NJC

New Journal of Chemistry

A journal for new directions in chemistry

rsc.li/njc

ISSN 1144-0546

ROYAL SOCIETY OF CHEMISTRY

PAPER

Iván González, Paulina Dreyse *et al.*

Substituent influence in phenanthroline-derived ancillary ligands on the excited state nature of novel cationic Ir(III) complexes

cnrs

NJC

PAPER

View Article Online
View Journal | View Issue

Cite this: *New J. Chem.*, 2018, 42, 6644

Substituent influence in phenanthroline-derived ancillary ligands on the excited state nature of novel cationic Ir(III) complexes†

Iván González, *[a] Mirco Natali, [b] Alan R. Cabrera, [c] Bárbara Loeb,[c] Jerónimo Maze[d] and Paulina Dreyse*[e]

In the quest for coordination compounds with potential applications in energy conversion processes, a new series of four Ir(III) complexes (**C1–4**) of the type $[Ir(R\text{-}ppy)_2(Ln)](PF_6)$, where R-ppy = 2-phenylpyridine (ppy) or 2,4-difluorophenylpyridine (F_2-ppy) and Ln = 1-methyl-1*H*-pyrazole[3′,4′:5,6]pyrazino[2,3-*f*]-[1,10]phenanthroline (**L1**) or thieno[3′,4′:5,6]pyrazino[2,3-*f*][1,10]phenanthroline (**L2**) has been synthesized. The photophysical properties of these compounds have been thoroughly characterized by both steady-state and time-resolved spectroscopic techniques, pointing out a complex interplay between excited states of different nature that plays a crucial role in the deactivation processes. In the case of complexes **C1–2** that feature the same **L1** ancillary ligand, the lowest excited states at room temperature are characterized by an admixture between the ^{3}MLCT/^{3}LLCT and ^{3}LC states, with an almost pure ^{3}LC character in **C2**. For **C3–4**, the admixture among charge-transfer and ligand-centred states is negligible, due to the appreciably low energy of the LC one, which, however, plays a non-innocent role in the deactivation pathway of the triplet charge-transfer emissive states of complexes **C3–4**. This work thus highlights the importance of a detailed comprehension of the photophysical properties of Ir(III) complexes in view of their use in energy transformation systems.

Received 19th January 2018,
Accepted 24th February 2018

DOI: 10.1039/c8nj00334c

rsc.li/njc

Introduction

Ir(III) cyclometalated complexes have been widely exploited in many research areas such as organic light-emitting diodes (OLEDs),[1] light-emitting electrochemical cells (LEECs),[2,3] luminescent sensors,[4–7] dye-sensitized solar cells (DSSCs),[8] non-linear optics (NLOs),[9,10] and as biological labeling agents.[11] All these applications are promoted due to the outstanding photophysical properties of these complexes, which involve high photostability, high photoluminescence quantum yields, and easy emission color tuning through modification of the ligand structures.[1,12] These unique features are attributable to the high spin–orbit coupling induced by the heavy iridium center, which promotes the direct population of spin-forbidden triplet excited states that may favorably decay *via* radiative routes.[1,3,13–18] In addition, the use of a third-row transition metal center increases the ligand-field splitting energy, making the metal center (MC) excited states less thermally accessible, thus avoiding non-radiative decays.[19–21]

Cationic cyclometalated Ir(III) complexes are typically represented as $[Ir(C^N)_2(N^N)]^+$, where C^N corresponds to the cyclometalating ligand, such as 2-phenylpyridine (ppy) and N^N represents a neutral polypyridine ancillary ligand, *e.g.*, 2,2′-bipyridine (bpy) or 1,10-phenanthroline (phen). The electronic transitions that these cationic iridium complexes can experience are metal-to-ligand charge-transfer (MLCT), ligand-to-ligand charge-transfer (LLCT, transition from cyclometalating ligand to ancillary ligand), and ligand-centered (LC); these transitions are responsible for the optical properties of these complexes, therefore, by the incorporation of electron withdrawing or donating groups on either ligands (N^N and/or C^N), the energy of the transition can be modulated.[19,22–24]

In general, in these complexes, the LUMO (lowest unoccupied molecular orbital) is usually located on the π* orbitals of the neutral (N^N) ancillary ligand, then, by modifying the substituents of the N^N ligand, it is possible to stabilize or destabilize mainly the LUMO. For example, Ir(III)-complexes with N^N ligands derived

[a] *Instituto de Investigación e Innovación en Salud, Facultad de Ciencias de la Salud, Universidad Central de Chile. Lord Cochrane 418, Santiago, Chile. E-mail: ivan.gonzalez@ucentral.cl*
[b] *Department of Chemical and Pharmaceutical Sciences, University of Ferrara, and Centro Interuniversitario per la Conversione dell'Energia Solare (SOLARCHEM), sez. di Ferrara, Via L. Borsari, 46, 44121 Ferrara, Italy*
[c] *Departamento de Química Inorgánica, Facultad de Química, Pontificia Universidad Católica de Chile. Vicuña Mackenna 4860, Macul, Santiago, Chile*
[d] *Facultad de Física, Pontificia Universidad Católica de Chile. Vicuña Mackenna 4860, Macul, Santiago, Chile*
[e] *Departamento de Química, Universidad Técnica Federico Santa María. Avenida España 1680, Valparaíso, Chile*

† Electronic supplementary information (ESI) available. See DOI: 10.1039/c8nj00334c

from pyrazino-[2,3-*f*][1,10]phenanthroline (ppl) show different electronic properties with or without carboxylate substituents linked to the pyrazine ring, showing that the increased electron-acceptor character of carboxylate ppl causes a decrease in the LUMO energy.[23–25] On the other hand, substituents in the C^N ligand can affect the energy of the HOMO (highest occupied molecular orbital), since the HOMO is typically an admixture of Ir dπ orbitals (t_{2g}) and π orbitals of the C^N. Therefore, modifications of the electronic nature of both ligands may have a profound impact on the absorption and emission energies of these complexes, which are assessed in consideration of specific applications.[24]

As far as polypyridine ligands are concerned, the ppl-based ligands have been extensively used in complexes of Ru(II), Os(II), Re(I), and Ir(III).[13,14,17,18,26] According to the ppl-structure, this ligand is considered to be constituted by two fragments, a portion that corresponds to the phen structure and a pyrazine (py) portion or its derivatives, depending on the ring or substituents linked to the py moiety.[14] This ligand is easily synthesized through a condensation reaction between diamine derivatives and a 1,10-phenanthroline-5,6-dione precursor.[14,27] In this context, this family of ligands offers a powerful strategy to modulate the electronic properties of complexes, due to the abundant library of diamines that can be employed.[14,27,28] One of the most popular polypyridine ligands of this sort is dipyrido[3,2-*a*:2′,3′-*c*]phenazine (dppz), which has been widely studied since the exploitation of the $[Ru(bpy)_2dppz]^{2+}$ complex as a spectroscopic probe in DNA intercalation, this advance being a precedent for further studies in this area.[29,30]

With the aim of increasing the library of cationic Ir(III) complexes with potential applications in diverse research fields, great efforts have been made with respect to the synthetic procedures of the ligands, which in many cases involve too complicated, high cost and low-yield routes. Taking into account the diversity of substituents that can be attached into the pyrazine fragment of the ppl ligand, without major difficulties, many and interesting coordination complexes have been synthesized.[13,31] Considering the interesting electronic structure of the ppl-based ligands for tuning the optical properties of Ir-complexes, and their simple synthetic procedures, in this work, the synthesis and photophysical characterization of a new series of cationic Ir(III) complexes (Scheme 1) $[Ir(R\text{-}ppy)_2(Ln)](PF_6)$ is described, where R-ppy = 2-phenylpyridine (ppy) or 2,4-difluorophenylpyridine (F_2-ppy) and Ln = 1-methyl-1*H*-pyrazolo [3′,4′:5,6]pyrazino [2,3-*f*][1,10]-phenanthroline (**L1**) or thieno [3′,4′:5,6]pyrazino [2,3-*f*][1,10]-phenanthroline (**L2**). A thorough photophysical and electrochemical investigation has been accomplished in order to fully understand the differences in terms of electronic properties within the series of complexes. The change of ring-substituents in the pyrazine moiety of the ppl-based ancillary ligand has a determining effect on the photophysical properties of these cationic Ir(III) complexes, promoting different contributions within the lowest excited states. The data provided may be interesting for the application of iridium(III) complexes in diverse research areas such as luminescent devices, sensors, and biology.

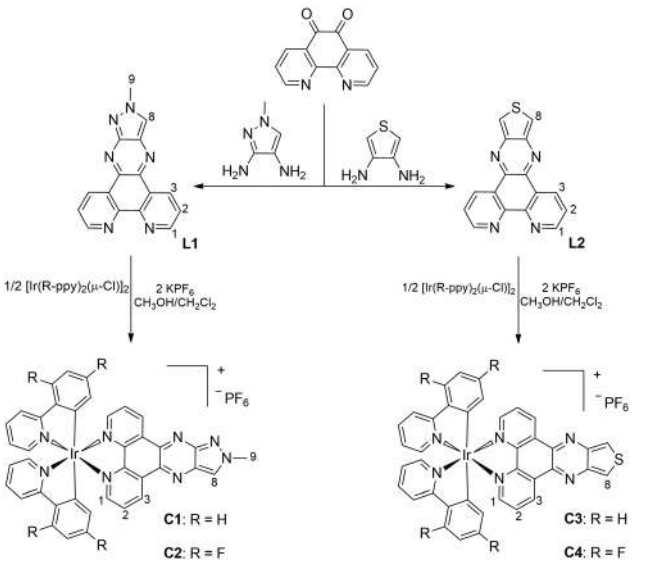

Scheme 1 Synthesis of the ligands (**L1–2**) and their respective Ir(III)-based complexes (**C1–4**).

Experimental section

General information and materials

All reagents and solvents commercially available were used as received unless otherwise specified. Iridium dimers ($[Ir(ppy)_2(\mu Cl)]_2$ and $[Ir(F_2\text{-}ppy)_2(\mu Cl)]_2$) were synthesized according to previous literature procedures.[12,13] NMR spectra were recorded on an NMR Bruker AV 400. Chemical shifts are given in parts per million relative to TMS [^{1}H and ^{13}C, $\delta(SiMe_4) = 0$] or an external standard [$\delta(CFCl_3) = 0$ for ^{19}F NMR]. Most NMR assignments were supported by additional 2D experiments. HR-MS(ESI) experiments were carried out using a Thermo Scientific Exactive Plus Orbitrap Spectrometer. The FT-IR spectra were recorded on a Bruker Vector-22 Spectrophotometer using KBr pellets. The UV-Vis spectra were registered using a Shimadzu UV-Vis-NIR 3101 PC spectrophotometer. Cyclic voltammograms were obtained using a PalmSens 3 Instruments Potentiostat in a three-electrode cell configuration with a platinum disc working electrode having a geometric area of 0.02 cm^2, a saturated Ag/AgCl reference electrode and a platinum wire counter electrode. All electrochemical measurements were carried out in anhydrous acetonitrile solutions of Ir(III) complexes (1 mM) with 0.1 M $TBAPF_6$ as supporting electrolyte at a scan rate of 0.1 V s^{-1}. Photoluminescence spectra were taken on an Edinburgh Instrument spectrofluorimeter. Solutions of the compounds were previously degassed with nitrogen for approximately 20 min. The emission quantum yields (Φ_{em}) were calculated according to the description of the literature.[9] 77 K luminescence measurements were performed by freezing alcoholic solutions (ethanol/methanol, 4/1) of complexes and ligands. Transient absorption measurements were performed with a custom laser spectrometer composed of a *Continuum Surelite II* Nd:YAG laser (FWHM = 6–8 ns) with a frequency doubled, (532 nm, 330 mJ) or tripled, (355 nm, 160 mJ) option, an *Applied Photophysics* xenon light source including a mod. 720 150W lamp housing, a mod. 620 power-controlled lamp supply

and a mod. 03-102 arc lamp pulser. Laser excitation was provided at 90° with respect to the white light probe beam. Light transmitted by the sample was focused onto the entrance slit of a 300 mm focal length *Acton SpectraPro 2300i* triple grating, flat field, double exit monochromator equipped with a photomultiplier detector (*Hamamatsu R3896*) and a *Princeton Instruments PIMAX II* gated intensified CCD camera, using a *RB Gen II* intensifier, a ST133 controller and a PTG pulser. Signals from the photomultiplier (kinetic traces) were processed by means of a *Teledyne LeCroy 604Zi* (400 MHz, 20 GS s^{-1}) digital oscilloscope.

Synthesis of L1 and L2

Ligand L1. 1,10-Phenanthroline-5,6-dione (1 eq.) was added to a solution of 1-methyl-1*H*-pyrazole-3,4-diamine (1 eq.) in absolute ethanol (100 mL). The mixture was refluxed for 1 h with vigorous stirring. The resulting solution was cooled to room temperature, filtered and the isolated solid was washed with cold ethanol. The filtrate was then diluted with water and extracted with CH_2Cl_2. The solvent was evaporated under vacuum to dryness. The resulting solid was dissolved in CH_2Cl_2 and precipitated with dry diethyl ether. The final product was isolated as an orange solid in 85% yield (231 mg, 0.81 mmol). ^{1}H NMR (400 MHz, DMSO-d_6, 298 K): δ/ppm = 9.53 (d, J = 8.1 Hz, 2H, H1), 9.45 (d, J = 8.1 Hz, 2H, H3), 8.99 (s, 1H, H8), 7.90 (broad, 2H, H2), 4.47 (s, 3H, H9). ^{13}C $\{^1$H$\}$ NMR (100 MHz, DMSO-d_6, 298 K): δ/ppm = 154.8, 150.8, 140.8, 133.0, 132.4, 131.5, 127.35, 125.2, 123.8, 41.4. HRMS(ESI): ($C_{16}H_{11}N_6$ $[M + H]^+$) calc.: 287.1045; found: 287.1027. FT-IR (KBr, ν/cm^{-1}) 1409 (C–N); 2916 (CH_3); 3014 (CH).

Ligand L2. 1,10-Phenanthroline-5,6-dione (1 eq.) was added to a solution of 3,4-diaminothiophene dihydrochloride (1 eq.) in absolute ethanol (100 mL). The mixture was refluxed for 1 h with vigorous stirring. The resulting solution was cooled to room temperature, filtered and the isolated solid was washed with cold ethanol. The filtrate was then diluted with water and extracted with CH_2Cl_2. The solvent was evaporated under vacuum to dryness. The resulting solid was dissolved in CH_2Cl_2 and precipitated with dry diethyl ether. The final product was isolated as an orange solid in 67% yield (184 mg, 0.63 mmol). ^{1}H NMR (400 MHz, DMSO-d_6, 298 K): δ/ppm = 9.44 (d, J = 8.1 Hz, 2H, H1), 9.20 (d, J = 4.5 Hz, 2H, H3), 8.28 (s, 2H, H8), 7.71 (dd, J = 4.5 Hz/8.1 Hz, 2H, H2). ^{13}C $\{^1$H$\}$ NMR (100 MHz, DMSO-d_6, 298 K): δ/ppm = 152.8, 148.9, 142.6, 141.6, 133.9, 128.2, 124.4, 117.4. HRMS(ESI): ($C_{16}H_9N_4S$ $[M + H]^+$) calc.: 289.0548; found: 289.1274. FT-IR (KBr, ν/cm^{-1}) 1116 (SC); 1508 (CN); 3078 (CH).

General synthetic procedure of complexes C1–4

The corresponding ligand (**L1** or **L2**) (2 eq.) and the bimetallic precursor ($[Ir(ppy)_2(\mu\text{-}Cl)]_2$ or $[Ir(F_2\text{-}ppy)_2(\mu\text{-}Cl)]_2$) (1 eq.) were dissolved in MeOH/CH_2Cl_2 (1 : 3). The mixture was stirred and refluxed for 12 h under a nitrogen atmosphere in darkness. Then, the volatiles were removed under vacuum and 500 mL of water was added to the crude product. The mixture was filtered and 2 equivalents of KPF_6 were added to the obtained solution, obtaining a yellow-orange precipitate. This solid was filtered and washed with water, dried and re-crystallized through CH_2Cl_2/diethyl ether diffusion. For additional experimental details, 2D NMR and assignments data, see ESI.†

Complex C1. Isolated as a yellow crystalline material in 71% yield (112 mg, 0.17 mmol). ^{1}H NMR (400 MHz, acetone-d_6, 298 K): δ/ppm = 9.77 (d, J = 8.1 Hz, 1H, H3a), 9.71 (d, J = 8.1 Hz, 1H, H3b), 9.16 (s, 1H, H8), 8.48 (dd, J = 5.1 Hz, 2H, H1a, H1b), 8.26 (d, J = 8.1 Hz, 2H, H10), 8.16 (td, J = 5.3 Hz/8.1 Hz, 2H, H2a, H2b), 7.94 (m, 4H, H11, H17), 7.88 (d, J = 5.8 Hz, 2H, H16), 7.09 (t, J = 7.5 Hz, 2H, H12), 7.00 (m, 4H, H13, H18), 6.46 (d, J = 7.5 Hz, 2H, H19), 4.61 (s, 3H, H9). ^{13}C $\{^1$H$\}$ NMR (100 MHz, acetone-d_6, 298 K): δ/ppm = 168.4, 153.1, 152.6, 151.0, 150.8, 150.5, 150.3, 149.4, 145.1, 140.5, 139.6, 138.3, 135.5, 134.9, 133.6, 132.6, 131.9, 131.2, 128.8, 127.1, 125.8, 124.6, 123.5, 120.7, 43.2. ^{19}F NMR (400 MHz, acetone-d_6, 298 K): δ/ppm = −70.1 (d, J^{F-P} = 712 Hz, PF_6). ^{31}P $\{^1$H$\}$ NMR (160 MHz, acetone-d_6, 298 K): δ/ppm = −144.2 (hept, J^{P-F} = 712 Hz, PF_6). HRMS(ESI) for ($C_{38}H_{26}IrN_8$ $[M]^+$) calc.: 787.1910; found: 787.1864. FT-IR (KBr, ν/cm^{-1}): 842, 557 (PF_6^-); 1476 (C–N); 2917 (CH_3).

Complex C2. Isolated as a yellow crystalline material in 73% yield (117 mg, 0.16 mmol). ^{1}H NMR (400 MHz, acetone-d_6, 298 K): δ/ppm = 9.74 (d, J = 8.2 Hz, 1H, H3a), 9.70 (d, J = 8.2 Hz, 1H, H3b), 9.14 (s, 1H, H8), 8.64 (d, J = 5.2 Hz, 1H, H1a), 8.61 (d, J = 5.2 Hz, 1H, H1b), 8.41 (d, J = 8.5 Hz, 2H, H10), 8.18 (m, 2H, H2a, H2b), 8.03 (t, J = 8.0 Hz, 2H, H11), 7.98 (broad, 2H, H13), 7.11 (t, J = 6.7 Hz, 2H, H12), 6.82 (t, J^{H-F} = 11.1 Hz, 2H, H17), 5.91 (d, J^{H-F} = 8.5 Hz, 2H, H19), 4.60 (s, 3H, H9). ^{13}C $\{^1$H$\}$ NMR (100 MHz, acetone-d_6, 298 K): δ/ppm = 163.5 (dd, J^{C-F} = 13.3 Hz/216.9 Hz), 163.2 (d, J^{C-F} = 4.5 Hz), 160.9 (dd, J^{C-F} = 12.5 Hz/220.2 Hz), 154.8 (d, J^{C-F} = 5.9 Hz), 153.6, 153.0, 151.3 (d, J^{C-F} = 11.1 Hz), 150.6, 150.3, 149.4, 140.7, 139.8, 138.7, 136.6, 135.9, 133.9, 132.6, 129.3, 129.0, 127.4, 125.1, 124.6 (d, J^{C-F} = 20.1 Hz), 114.8 (d, J^{C-F} = 17.1 Hz), 99.8 (t, J^{C-F} = 26.9 Hz), 43.2. ^{19}F NMR (400 MHz, acetone-d_6, 298 K): δ/ppm = −70.2 (d, J^{F-P} = 712 Hz, PF_6), −106.5 (t, J^{F-H} = 8.0 Hz, F-C18), −108.7 (t, J^{F-H} = 11.0 Hz, F-C16). ^{31}P $\{^1$H$\}$ NMR (160 MHz, acetone-d_6, 298 K): δ/ppm = −144.2 (hept, J^{P-F} = 712 Hz, PF_6). HRMS HRMS(ESI) for ($C_{38}H_{22}F_4IrN_8$ $[M]^+$) calc.: 859.1533; found: 859.1473. FT-IR (KBr, ν/cm^{-1}) 845, 557 (PF_6^-); 1478 (CN); 2919 (CH_3).

Complex C3. Isolated as a yellow crystalline material in 65% yield (52 mg, 0.05 mmol). ^{1}H NMR (400 MHz, acetone-d_6, 298 K): δ/ppm = 9.49 (d, J = 8.3 Hz, 2H, H3), 8.58 (s, 2H, H8), 8.26 (d, J = 5.3 Hz, 2H, H1), 8.06 (d, J = 8.3 Hz, 2H, H9), 7.95 (dd, J = 5.3 Hz/8.3 Hz, 2H, H2), 7.75 (t, J = 8.0 Hz, 2H, H10), 7.70 (m, 4H, H16, H15), 6.89 (m, 2H, H11), 6.84 (m, 2H, H12), 6.79 (m, 2H, H17), 6.24 (d, J = 7.6 Hz, 2H, H18). ^{13}C $\{^1$H$\}$ NMR (100 MHz, acetone-d_6, 298 K): δ/ppm = 166.8, 151.5, 150.1, 149.7, 149.6, 144.0, 141.4, 139.8, 138.8, 134.8, 131.5, 131.1, 130.3, 128.5, 125.1, 123.8, 122.5, 120.1, 120.0. ^{19}F NMR (400 MHz, acetone-d_6, 298 K): δ/ppm = −70.2 (d, J^{F-P} = 712 Hz, PF_6). ^{31}P $\{^1$H$\}$ NMR (160 MHz, acetone-d_6, 298 K): δ/ppm = −144.2 (hept, J^{P-F} = 712 Hz, PF_6). HRMS(ESI) for ($C_{38}H_{24}IrN_6S$ $[M]^+$) calc.: 789.1412; found: 789.1371. FT-IR (KBr, ν/cm^{-1}) 843, 557 (PF_6^-); 1163 (SC); 1477 (CN).

Complex C4. Isolated as a yellow crystalline material in 68% yield (57 mg, 0.06 mmol). ^{1}H NMR (400 MHz, acetone-d_6,

298 K): δ/ppm = 9.65 (d, J = 8.2 Hz, 2H, H3), 8.72 (s, 2H, H8), 8.59 (d, J = 5.1 Hz, 2H, H1), 8.41 (d, J = 8.3 Hz, 2H, H9), 8.14 (dd, J = 5.3 Hz/7.8 Hz, 2H, H2), 8.03 (t, J = 7.8 Hz, 2H, H10), 8.00 (t, J = 5.6 Hz, 2H, H12), 7.15 (t, J = 6.6 Hz, 2H, H11), 6.81 (dd, J^{H-F} = 9.7 Hz/11.4 Hz, 2H, H16), 5.91 (d, J^{H-F} = 8.6 Hz, 2H, H18). ^{13}C {^{1}H} NMR (100 MHz, acetone-d_6, 298 K): δ/ppm = 164.5 (dd, J^{C-F} = 13.3 Hz/255.0 Hz,), 164.6 (d, J^{C-F} = 7.0 Hz), 162.3 (dd, J^{C-F} = 12.5 Hz/258.0 Hz), 154.7 (d, J^{C-F} = 6.6 Hz), 153.6, 151.1, 151.1, 142.9, 140.7, 140.6, 136.6, 133.1, 129.6, 129.0 (d, J^{C-F} = 4.5 Hz), 125.0, 124.5 (d, J^{C-F} = 20.1 Hz), 120.6, 114.8 (d, J^{C-F} = 18.0 Hz), 99.8 (t, J^{C-F} = 27.1 Hz). ^{19}F NMR (400 MHz, acetone-d_6, 298 K): δ/ppm = −72.6 (d, J^{F-P} = 708 Hz, PF_6), −107.7 (dd, J^{F-H} = 9.3 Hz/18.8 Hz, F-C17), −110.0 (t, J^{F-H} = 11.6 Hz, F-C15). ^{31}P {^{1}H} NMR (160 MHz, acetone-d_6, 298 K): δ/ppm = −144.4 (hept, J^{P-F} = 708 Hz, PF_6). HRMS(ESI) for ($C_{38}H_{20}F_4IrN_6S$ $[M]^+$) calc.: 861.1036; found: 861.1036. FT-IR (KBr, ν/cm^{-1}) 845; 557 (PF_6^-); 1168 (SC); 1477 (CN).

Results and discussion

Synthesis and characterization

Four new cationic cyclometalated Ir(III) complexes (**C1–4**) were synthesized according to literature methods.[32–34] In these complexes, two N^N ancillary ligands derived from 1,10-phenantroline were used, obtained by a nucleophilic substitution reaction between equimolar amounts of 1,10-phenanthroline-5,6-dione and the respective 3,4-diamine derivatives, obtaining the ligands **L1** (1-methyl-1*H*-pyrazolo[3′,4′:5,6]pyrazino[2,3-*f*][1,10]phenanthroline) and **L2** (thieno[3′,4′:5,6]pyrazino[2,3-*f*][1,10]phenanthroline) (Scheme 1), respectively, in good yield, which were characterized by NMR, FT-IR, and high resolution mass spectrometry (HR-MS(ESI)) analyses. Complexes **C1–4** were obtained in a two-step reaction: (1) the mixture of two molar equivalents of N^N ligand (**L1–2**) with one molar equivalent of the bimetallic Ir(III) precursor $[Ir(R\text{-}ppy)_2(\mu\text{-}Cl)]_2$ in CH_3OH/CH_2Cl_2, followed by (2) the addition of two molar equivalents of KPF_6 (see Scheme 1) to achieve the four cationic Ir(III) complexes in high yields. All complexes were air and thermally stable, in solution as well as in the solid state, and were fully characterized by NMR, FT-IR, and HR-MS(ESI).

The spectroscopic characterization of complexes **C1–4** is consistent with a single Ir(III) metal center coordinated by two phenylpyridine ligands (R-ppy) and one phenanthroline-based ancillary ligand (**L1** or **L2**). The ^{1}H NMR spectra of the complexes exhibited a low-field displacement of all chemical shifts, in comparison with their corresponding free N^N ligands, *e.g.* the chemical shift of H_2 **L1** (see Scheme 1 for proton labeling) displaces from 7.90 ppm to 8.16 and 8.18 ppm in **C1** and **C2**, respectively. This behavior is due to a magnetic de-shielding effect promoted by the Ir(III) metal center and is in agreement with the electron donating character of the N^N ligands. In addition, the electron withdrawing fluorine atom in the phenylpyridine of the complexes exerted the higher electronic effect over the ancillary ligand, as expected. Nevertheless, the electronic effect induced by the phenylpyridine substituents over **L1** and **L2** coordinated ligands is more prominent in **C3–C4** complexes than in **C1–C2**, *e.g.* the difference in the chemical shifts of H_8 between **C3** and **C4** is 0.14 ppm, meanwhile between **C1** and **C2**, it is 0.02 ppm. This can be attributed to a higher electron density removal in **L2** ligand towards the Ir(III), affected by the nature of the ppy ligand, than from the **L1** ligand. This is in agreement with a more conjugated aromatic portion between the metal center and the thiophene portion in **L2**. On the other hand, all complexes exhibit a similar chemical shift for the PF_6^- counter-ion in the ^{19}F and ^{31}P NMR spectra (^{19}F: −70.2 ppm as a doublet (J^{F-P} = 712 Hz); ^{31}P: −144.2 ppm as a septet (J^{P-F} = 713 Hz)). For further information, including 2D NMR and assignment data, see the ESI.†

Electrochemical properties

The electrochemical behavior of the complexes **C1–4** was determined by cyclic voltammetry (CV). The voltammetric profiles of the complexes are shown in Fig. 1. The experiments were carried out using Ag/AgCl as the reference electrode and acetonitrile solutions of the compounds. The assignments of the redox processes were based on comparisons with electrochemical data previously reported for similar ligands and Ir(III) complexes.[23,25,35–38] The values of the oxidation and reduction processes are collected in Table 1. The cyclic voltammograms

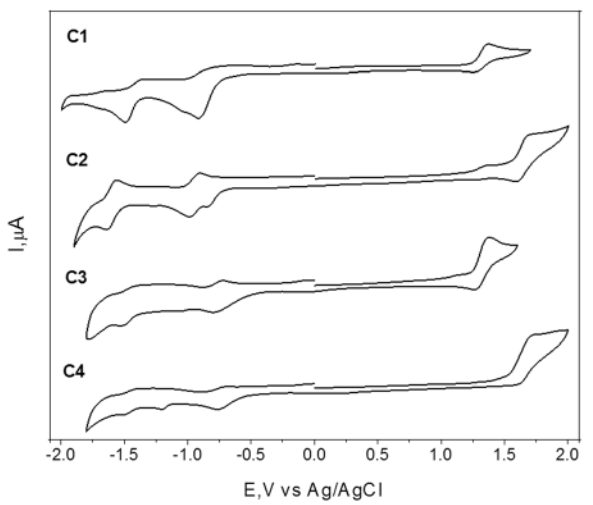

Fig. 1 Cyclic voltammetric profiles recorded in CH_3CN solution at 0.1 V s^{-1} for Ir(III) complexes **C1–4**.

Table 1 Values of the absorption and redox processes for complexes **C1–4**

	λ_{abs}/nm[a]	ε[a]/M^{-1} cm^{-1}	E_{ox}[b]/V	E_{red}[b]/V
C1	380	33 300	1.31	−0.91; −1.48
C2	365	23 951	1.64	−0.87; −0.99; −1.65
C3	370	14 895	1.32	−0.79; −1.52
	395	11 350		
C4	360	12 753	1.74	−0.76; −1.52
	387	8702		

[a] In acetonitrile solution at room temperature. [b] $E_{ox} = E_{pa}$ and $E_{red} = E_{pc}$; acetonitrile/TBAPF$_6$ 0.1 M, *vs.* Ag/AgCl.

of the complexes towards positive potentials exhibit a quasi-reversible redox process, which is attributed to the Ir(IV)/Ir(III) couple together with a contribution of the oxidation from the phenyl π orbital of the cyclometalating (C^N) ligands.[19,23,25,35,37] The oxidation potential values of the complexes with the F_2-ppy ligand are more positive than those of **C1** and **C3**. This behavior is rather expected, considering the electron-withdrawing nature of the F_2-ppy ligand.[19,25,39] On the other hand, at negative potentials, it is possible to observe many reduction processes that are attributable to the ancillary ligands, as described for other transition metal complexes with these kinds of polypyridine ligands.[13,38,40] In the case of complexes **C1** and **C2**, the first reduction process takes place at a more negative potential compared to complexes **C3** and **C4**. In accordance with these characteristics, the first reduction process can reasonably be attributed to the reduction of the pyrazine fragment of the ancillary ligand, whereas the remaining reduction processes can be ascribed to the phenantroline part. Similar results have been reported for the reduction potentials of Re(I), Pd(II), and Ir(III) complexes with dppz based ligands.[13,38,40]

Absorption properties

The absorption spectra of the complexes and N^N ligands in acetonitrile solutions are shown in Fig. 2. The absorption maxima and molar extinction coefficients of the complexes are summarized in Table 1. For **L1** and **L2** (see Fig. 2A), intense absorption bands in the UV region (250–330 nm) are ascribable to π → π* transitions, according to the description of similar systems.[14,33] The lowest energy transitions at *ca.* 350 nm can be tentatively assigned, at least for ligand **L2**, as intraligand charge transfer transitions (ILCT), as suggested by Rasmussen, *et al.*[33] In the case of the absorption spectra of the complexes (see Fig. 2B), the intense bands at approximately 250–320 nm correspond to ligand-centered (LC) transitions (π → π*), attributable to the ancillary and cyclometalating ligands. For **C3** and **C4**, it is possible to observe that these absorption bands have many vibrational components related mainly to **L2**. While in **C1** and **C2**, an intense and broad band is observed, with a molar absorption coefficient in the order of 1.3×10^5 and 9×10^4 M^{-1} cm^{-1}, respectively, which is consistent with the absorption profiles of the free ligands. Furthermore, the complexes display less intense absorption shoulders at around 350–410 nm, which are ascribable to both spin-allowed metal-to-ligand (^{1}MLCT) and ligand-to-ligand (^{1}LLCT) charge transfers ($\varepsilon > 1 \times 10^4$ M^{-1} cm^{-1}). The energy and shape of these transitions are characteristic of $[Ir(C^N)_2(N^N)]^+$ complexes.[13,23,24] These MLCT/LLCT bands are likely superimposed onto the ILCT transitions observed in the free ligands, although metal coordination may slightly change the actual energy of the latter. This behavior has been observed in a similar system based on the Re(I) complex with dppz, in which the spectral properties were dominated by very strong transitions related to the quinoxaline portion of the ligand.[34,41]

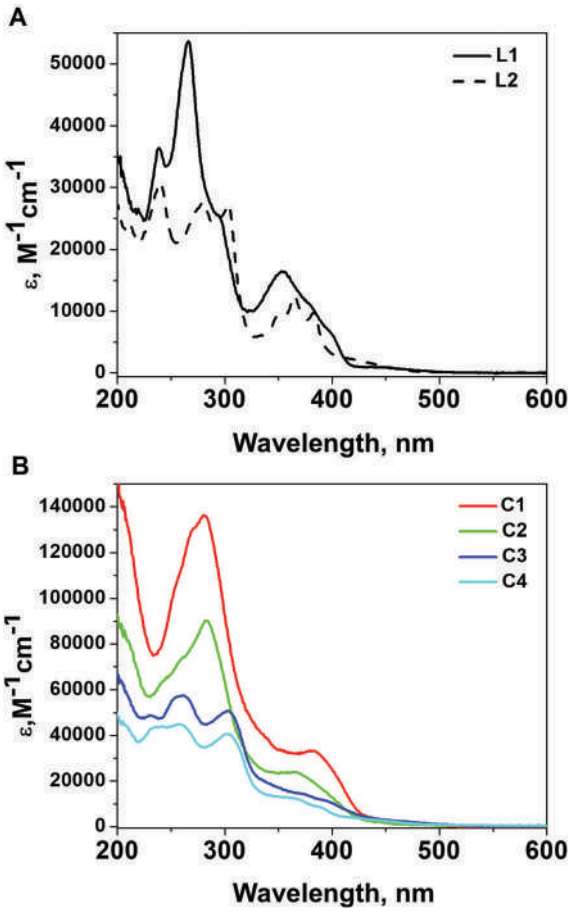

Fig. 2 Absorption spectra in acetonitrile solutions of the: (A) ligands (**L1–2**) and (B) their respective Ir(III)-based complexes (**C1–4**).

The absorption spectra of the ancillary ligands and complexes were also registered in dichloromethane solutions (data are summarized in the ESI,† Fig. S13). For the ligands, only small differences in the absorption maxima induced by the solvent polarity were observed. The complexes showed red-shifts in the maximum of the lower-energy bands when going from acetonitrile to dichloromethane, thus corroborating the charge transfer (MLCT/LLCT) character of these transitions.[42–44]

Luminescence properties

The photoluminescence properties of the ancillary ligands and complexes were studied in fluid solution and in a glassy matrix at 77 K. All the relevant data are summarized in Table 2.

The luminescence of the ancillary ligands **L1** and **L2** was first measured in acetonitrile solution and upon addition of $ZnClO_4$ in order to simulate the coordinated situation within the metal complex (see ESI,† Fig. S14). Excitation of **L1** and **L2** is followed by a broad, featureless emission with maxima at 438 and 535 nm, respectively, which shift towards lower energy in the presence of zinc (454 nm and 559 nm for **L1** and **L2**, respectively), possibly associated with the extended π-electron conjugation system formed upon coordination,[45] and are attributable to ligand-based fluorescence.[33,46]

When probed in a glassy matrix at 77 K, beside the fluorescence signal that appears as a shoulder at higher energy, the ancillary ligand **L1** in the presence of $ZnClO_4$ displays an intense, structured emission with relative maxima at 555 and 605 nm (Fig. S15, ESI†) that can be reasonably assigned to the ligand phosphorescence. On the other hand, the ancillary ligand **L2** with Zn^{2+} ions in the

Table 2 Photophysical properties of complexes **C1–4**[a]

	CH_3CN solution			CH_2Cl_2 solution			77 K glassy matrix	
	λ_{em}/nm	Φ^b	τ^c/μs	λ_{em}/nm	Φ^b	τ^c/μs	λ_{em}/nm	τ^c/μs
C1	738	0.004	0.177	640	0.092	2.0	564, 612, 670	4.07 (83%), 1610 (17%)
C2	573, 620	0.010	0.967 (92%), 24.3 (8%)	572, 620	0.031	0.983 (95%), 17.4 (5%)	564, 612, 670	5.80 (84%), 6920 (16%)
C3	620	0.010	0.303	603	0.030	0.521	550	3.50
C4	551	0.027	0.862	534	0.031	0.786	497	4.81

[a] Excitation between 380–400 nm. [b] Obtained with relative method using $Ru(bpy)_3Cl_2 \cdot 6H_2O$ as actinometer (Φ = 0.04 in air-equilibrated water solution).[47] [c] Excitation at 355 nm; detection at λ_{em}.

alcoholic glassy matrix at 77 K shows only the emission feature (maximum at 545 nm) compatible with the ligand fluorescence; the related phosphorescence, if any, likely occurs at longer wavelengths than experimentally measured.

In degassed acetonitrile solutions at room temperature (Fig. 3A), complexes **C1**, **C3**, and **C4** show a broad emission profile mainly attributable, at first glance, to radiative deactivations from the triplet metal-to-ligand or ligand-to-ligand charge-transfer (^{3}MLCT or ^{3}LLCT) excited states or a mixture of both, as has been described for cationic Ir(III) complexes with phenanthroline derivatives as ancillary ligands.[13,24,48–50] The emissions are consistent with the energy of the MLCT/LLCT transitions as observed in the absorption measurements (see Fig. 2 and Table 1).

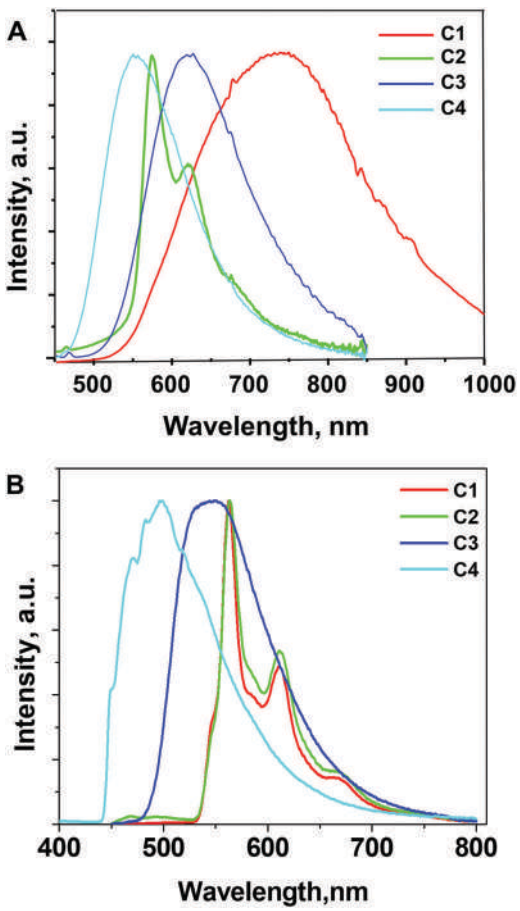

Fig. 3 Normalized photoluminescence spectra of Ir(III) complexes in (A) acetonitrile solution and (B) in an alcoholic glassy matrix at 77 K.

From comparison with the emission properties of related ruthenium(II) complexes bearing fused polypyridine ligands,[51] the observed emission (with the exception of **C2**) most likely arises from triplet MLCT/LLCT excited states with an electron localized onto the phenanthroline moiety of the ancillary ligands rather than the terminal pyrazine fraction, although the electronic effect exerted by the latter fragment is seen to play an important role as well. Complex **C2**, on the other hand, shows a prominent, structured emission with maxima at 573 and 620 nm, suggesting a different contribution, most likely of ligand-centered (LC) nature. In complexes **C2** and **C4**, the emission patterns are blue-shifted with respect to those of **C1** and **C3**, respectively. This is consistent with the presence of F_2-ppy in lieu of the ppy cyclometalating ligand, which leads to the stabilization of the HOMO, thus generating an increase in the HOMO–LUMO gap, as typically observed with related iridium(III) complexes.[52–55] This effect is particularly relevant in the comparison of complexes **C1** and **C2** in which the change from ppy to F_2-ppy ligand causes a switch from MLCT/LLCT to LC emission. When the solvent is changed to dichloromethane, complexes **C1**, **C3**, and **C4** exhibit similar, broad luminescence features (Fig. S13, ESI†) only differing by an appreciable blue-shift of the emission maxima. This observation speaks in favor of an important MLCT/LLCT contribution in the emission since the decrease in solvent polarity on going from acetonitrile to dichloromethane brings about a destabilization (*i.e.*, a shift towards higher energy) of the triplet charge transfer emissive state.[56–58] Conversely, the almost identical spectral shape and energy of the luminescence of complex **C2** in both acetonitrile and dichloromethane solutions confirms the predominant contribution from a triplet LC excited state. Quantum yields between 0.4 and 2.7% were measured in acetonitrile solution, while these values appreciably increase on going to the less polar dichloromethane reaching quantum yields between 3.0 and 9.2% (Table 2). In the case of MLCT/LLCT emitters such as **C1**, **C3**, and **C4**, the gain in emission yield upon change of the solvent can be at least qualitatively ascribed to energy-gap-law arguments, whereas in the case of **C2**, it can likely be ascribed to the increased contribution of the LC state in the emissive state. The decay of the photoluminescence was then monitored by time-resolved emission experiments. At room temperature in both degassed acetonitrile and dichloromethane solutions (Table 2), complexes **C1**, **C3**, and **C4** show a single-exponential decay with lifetimes between a hundred ns and a few μs, which is typical of MLCT (or mixed MLCT/LLCT) phosphorescence.[50]

A slight increase is generally observed on going from acetonitrile to dichloromethane solution consistent with the enhancement of the luminescence quantum yield previously discussed. A substantial increase in lifetime is observed, however, for complex **C1** only that most likely arises from the destabilization of the triplet MLCT/LLCT state when moving to the less polar environment and the concurrent improved mixing of the triplet LC excited state within the emitting manifold. On the other hand, in the case of complex **C2**, a biexponential decay is recorded with a longer component in the ten μs time scale. The presence of two time components in the emission decay of complex **C2** very likely reflects the kinetics of the equilibration processes between the triplet LC and the closely lying ^{3}MLCT/^{3}LLCT excited state.[59]

The photoluminescence spectra registered in a 4/1 ethanol/methanol glass at 77 K (Fig. 3B) show the same structured spectral profile in the case of both complexes **C1** and **C2** that strongly resembles the phosphorescence profile of ligand **L1** (Fig. S15, ESI†) and can be thus compatible with a major contribution from a ^{3}LC excited state. The switch from mainly MLCT/LLCT to LC emission in the case of complex **C1** with the rigidity of the medium can be explained considering the destabilization of the ^{3}MLCT/^{3}LLCT state occurring in the glassy matrix at 77 K, which rises above the ^{3}LC one with respect to room-temperature, fluid conditions. This observation is further substantiated by the emission decays of complexes **C1** and **C2** measured in this rigid matrix, which show a second-order behavior with the second component reaching the ms time scale (Table 2), typical of ligand-based triplet emitters.[59] The presence of two time components in the decay can be explained by the kinetics of the equilibration process between the emissive LC and the closely lying ^{3}MLCT/^{3}LLCT excited state. Conversely, for complexes **C3** and **C4**, the emission at 77 K shows featureless spectral profiles, which are compatible with a major contribution from the MLCT/LLCT excited states. The blue-shift observed with respect to the emission in solution is fully consistent with this notion and is explained on the basis of the so-called rigidochromic effect.[58–60] The single exponential decay with μs lifetime measured by the time-resolved emission technique still confirms the latter attribution. This situation can be explained considering the substantially lower energy of the triplet LC excited state of the ancillary ligand **L2** (as possibly hypothesized from emission measurements on the free ligand and literature data,[33] see above) that prevents any mixing with the emitting charge-transfer state.

Transient absorption spectroscopy

In order to obtain a clearer picture concerning the photophysical behavior of complexes **C1–4**, time-resolved absorption spectroscopy measurements with time-resolution from ns to ms were performed in both acetonitrile and dichloromethane solutions. Upon 355 nm excitation of complex **C1**, a transient spectrum is immediately detected after the laser pulse (0.02 μs time-delay, Fig. 4A, black trace) that displays an absorption with a peak at 470 nm and a shoulder at *ca.* 550 nm with a tail at longer wavelengths and can be reasonably assigned to the lowest-lying excited state of the metal complex with triplet spin multiplicity.

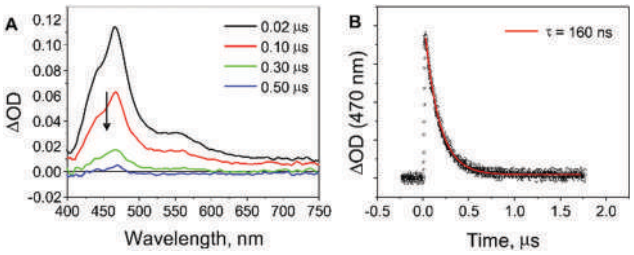

Fig. 4 (A) Transient absorption spectra at different time-delays obtained on complex **C1** in acetonitrile by laser flash photolysis (excitation at 355 nm) and (B) kinetic analysis at 470 nm with related fitting.

This transient spectrum decays monotonically to the baseline (Fig. 4A) with kinetics that are dependent on oxygen concentration, thus confirming the triplet nature of the transient species. A first-order kinetics treatment can be applied to the decay-associated kinetics (Fig. 4B) and a lifetime of τ = 160 ns can be estimated in a nitrogen-purged solution. A similar behaviour is also observed in dichloromethane where a similar spectrum undergoes a monotonic decay with a lifetime of τ = 1.9 μs under deoxygenated conditions (Fig. S16, ESI†).

When complex **C2** is studied by laser flash photolysis, a comparable spectrum with respect to the one observed for complex **C1** is promptly detected (Fig. 5A, black trace), ascribable to the lowest-lying triplet excited state. This latter spectrum then undergoes a monotonic decay to the baseline (Fig. 5A) with a lifetime of τ = 19 μs in deoxygenated acetonitrile (Fig. 5B). Similar spectral changes and a comparable decay (τ = 20 μs) are seen for complex **C2** when experimented in dichloromethane solution (Fig. S17, ESI†).

Interestingly, the transient spectra observed in the laser flash photolysis of both complexes **C1** and **C2** are comparable in shape with the transient spectrum associated with the triplet excited state of the ligand as obtained by the photolysis of the ancillary ligand **L1** in the presence of zinc(II) cations (Fig. S18, ESI†). This thus suggests that the transient species associated with the differential spectra of both **C1** and **C2** (Fig. 4A and 5A, respectively) does correspond in both cases to a triplet excited state with a considerable ligand-centered (^{3}LC) character, as previously inferred based on simple emission data (see above).

Additional information can then be obtained comparing the transient absorption lifetimes with those measured by time-resolved emission. In the case of complex **C1**, the lifetime of the

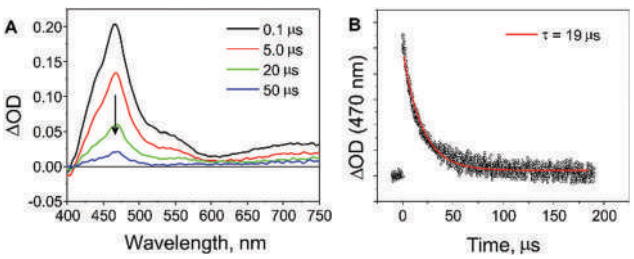

Fig. 5 (A) Transient absorption spectra at different time-delays obtained on complex **C2** in acetonitrile by laser flash photolysis (excitation at 355 nm) and (B) kinetic analysis at 470 nm with related fitting.

transient species matches the emission lifetime (see above, Table 2), thus suggesting that a ligand-centered character is in fact present together with the MLCT/LLCT character in the luminescent excited state of **C1** and that the equilibration between ^{3}MLCT/^{3}LLCT and ^{3}LC excited states is sufficiently faster than it can be detected. The elongation of the lifetime on going from acetonitrile to dichloromethane is consistent with this notion and can be understood considering an enhanced contribution of the ligand-centered character within the triplet emitting admixture (^{3}LC/^{3}MLCT/^{3}LLCT) caused by the destabilization of the MLCT/LLCT state by lowering the solvent polarity. On the other hand, in the case of complex **C2**, the decay of the transient species, as measured by transient absorption spectroscopy, is monotonic and slower (tens μs time-scale) and matches only the longer component of the luminescence decay as measured by time-resolved emission (Table 2). No trace is observed in the transient absorption experiments of the fast decaying component. This experimental evidence can be tentatively rationalized considering a lowest-lying, emitting ^{3}LC excited state in slow, thermal equilibrium with a closely lying excited state (presumably of MLCT/LLCT character) in that the short lifetime (measured by emission only, *ca.* 1 μs) is related to the kinetics of the equilibration process, while the long component (measured by both emission and transient absorption, tens μs time-scale) corresponds to the decay of the ^{3}LC excited state to the ground state.[59]

The transient absorption behavior of the remaining complexes **C3** and **C4** is apparently more intricate than those of **C1** and **C2**. Upon 355 nm excitation of complex **C3**, a biphasic behavior is observed in nitrogen-purged acetonitrile solution (Fig. 6). The prompt spectrum (measured at 20 ns after the laser pulse, black trace of Fig. 6A) displays a prominent absorption centered at 500 nm, and an apparent bleach at $\lambda > 550$ nm, which can be directly associated with a triplet MLCT/LLCT excited state being comparable in shape with that of the triplet MLCT states of related

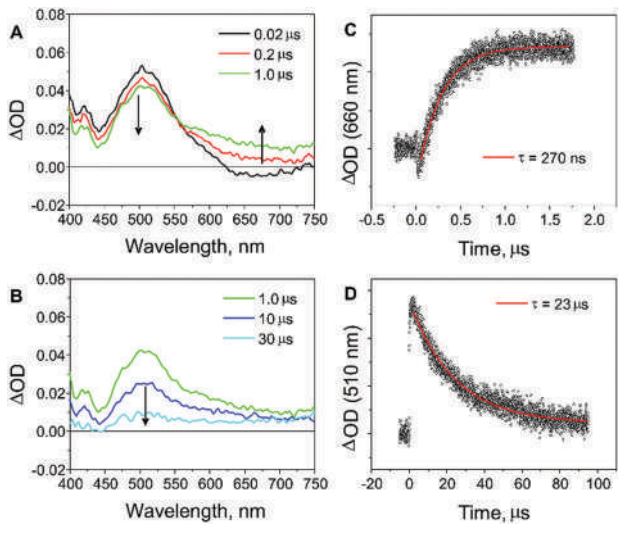

Fig. 6 (A) Transient absorption spectra obtained on complex **C3** in acetonitrile by laser flash photolysis (excitation at 355 nm) between 0.02–1.0 μs and (B) 1.0–30 μs; (C) kinetic analyses at 660 nm and (D) 510 nm with related exponential fitting.

iridium(III) complexes.[61] The presence of the apparent bleach at around 600–650 nm, attributable to the emission, is consistent with this hypothesis. After *ca.* 2 μs (Fig. 6A), a spectral evolution is observed wherein the absorption feature undergoes a slight decay with the maximum shifting to 510 nm and, concurrently, the ΔOD values in the red portion of the spectrum increase (isosbestic point at 554 nm). Interestingly, the spectrum thus obtained (1 μs time delay, green trace in Fig. 6A and B) perfectly matches the transient signal measured by laser flash photolysis of the ancillary ligand **L2** with $ZnClO_4$ (Fig. S19, ESI†) and can be attributed to a ligand-centered triplet excited state. This latter spectrum then undergoes decay to the baseline (Fig. 6B). The first spectral evolution (Fig. 6A) takes place with a time-constant of τ = 270 ns (Fig. 6C) and is compatible with the excited state lifetime as measured by time-resolved emission (Table 2). Therefore, supported also by the spectral attributions previously made, it can easily be associated with the deactivation of the emitting MLCT/LLCT excited state to yield a ligand-localized triplet excited state (^{3}LC).

The second process (spectral evolution of Fig. 6B) that occurs with a time-constant of τ = 23 μs (Fig. 6D) can then be ascribed to the ground-state decay of the ligand-centered excited state *via* non-radiative routes. Similar spectral changes are also detected in dichloromethane solution (Fig. S20, ESI†), only differing in the presence of a preceding, fast process, likely attributable to a ^{3}MLCT/^{3}LLCT excited state equilibration (herein slower than in acetonitrile), and in the kinetics of the remaining processes (τ_1 = 615 ns and τ_2 = 18 μs, for MLCT/LLCT and LC deactivations, respectively).

Transient absorption spectroscopy studies on complex **C4** were finally performed. When obtained in acetonitrile solution (Fig. 7), the prompt spectrum, measured at 20 ns time-delay after excitation (Fig. 7A, black trace), displays a prominent absorption with two maxima at 420 and 480 nm, an apparent bleach at *ca.* 550 nm, and a broad absorption above 600 nm. During the first hundred ns (Fig. 7A), the absorption signals in both the blue and red regions of the spectrum undergo a partial decay to yield a new spectrum with a maximum at 485 nm, while maintaining the bleaching at *ca.* 550 nm. The spectrum obtained herein (Fig. 7A and B, green trace) is comparable to that of triplet MLCT excited states of similar iridium(III) complexes reported in the literature[61] as well as to the prompt spectrum measured in complex **C3** (see above, Fig. 6A, black trace), differing mainly by the bleach at *ca.* 550 nm attributable to the emission (here, blue-shifted with respect to **C4**). Thus, this spectral evolution (Fig. 7A), taking place with a time-constant of τ = 45 ns (Fig. 7D), can be attributed, on a tentative basis, to an equilibration within the triplet MLCT/LLCT manifold (as previously inferred for **C3** in dichloromethane). Subsequently (within *ca.* 2 μs, Fig. 7B), a slight decrease in the higher-energy excited-state absorption is observed with the concomitant increase in the ΔOD signal between 500 and 600 nm (isosbestic point at 490 nm) leaving a transient absorption with the maximum at *ca.* 510 nm, compatible with the spectrum of the ligand-centered triplet excited state (Fig. S19, ESI†). Accordingly, the similarity of these spectral changes with those observed in complex **C3** (see above, Fig. 6A) may reasonably point toward the assignment of the process described in Fig. 7B

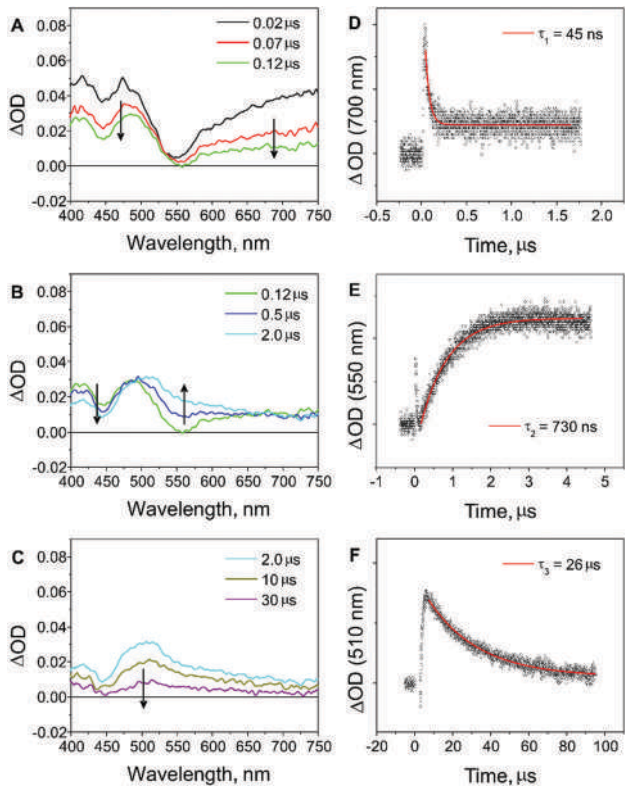

Fig. 7 (A) Transient absorption spectra obtained on complex **C4** in acetonitrile by laser flash photolysis (excitation at 355 nm) between 0.02–0.12 μs, (B) 0.12–2.0 μs, and (C) 2.0–30 μs; (D) kinetic analyses at 700 nm, (E) 550 nm, and (F) 510 nm with related exponential fitting.

to the decay of the triplet MLCT/LLCT state to give a ligand-centered (^{3}LC) excited state. This process, taking place with a time-constant of τ = 730 ns (Fig. 7E), displays a kinetics that is compatible with the emission lifetime measured by time-resolved emission and may further sustain the attribution made. Finally, the transient spectrum with the maximum at *ca.* 510 nm decays to the baseline (Fig. 7C), representing the deactivation of the so-formed, ligand-localized triplet excited state toward the ground state. A time-constant of τ = 26 μs can be estimated from the fitting of the kinetic trace measured in its absorption maximum (Fig. 7F). Similar transient absorption dynamics are observed for complex **C4** in dichloromethane solution (Fig. S21, ESI†) that only differ, with respect to acetonitrile, by a somewhat more pronounced MLCT/LLCT equilibration process and by the kinetics of all three processes (τ_1 = 40 ns, τ_2 = 1.1 μs, and τ_3 = 32 μs).

Summary of the photophysical behavior

The photophysical behaviour of all metal complexes in fluid solutions at room temperature can be rationalized by the following considerations, which are summarized in the energy level diagrams of Fig. 8. The photophysics of complex **C1** is dictated by an interplay of triplet MLCT/LLCT and LC excited states in fast equilibrium due to the comparable energies (Fig. 8A). This excited state admixture is responsible for the observed emission. The amount of MLCT/LLCT and LC contributions can be modulated by varying the solvent polarity, which affects only the relative energy of the charge transfer states, resulting in both higher excited state lifetimes and emission yields when moving from acetonitrile to dichloromethane. In the case of complex **C2**, the substitution of the ppy ligands with fluorine-based ones, F_2-ppy, shifts the MLCT/LLCT excited state towards higher energies with the triplet LC state now becoming the lowest excited state in both acetonitrile and dichloromethane, as monitored by steady-state emission.

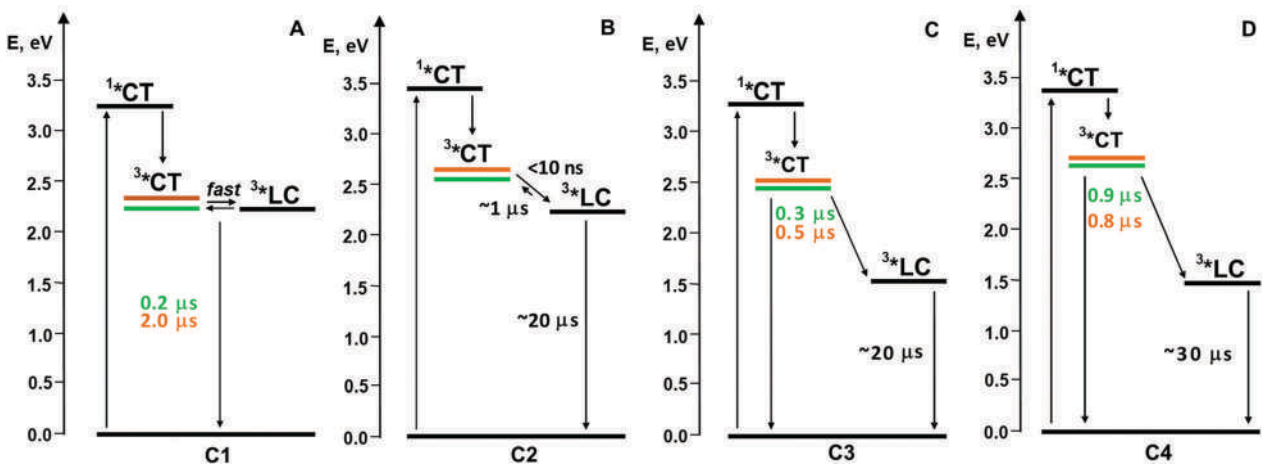

Fig. 8 Energy level diagram of complexes (A) **C1**, (B) **C2**, (C) **C3** and (D) **C4** with related processes (at room temperature) and time-constants (taken from emission data for CT states and from transient absorption for LC ones). Abbreviations: CT = MLCT/LLCT, LC = ligand-centered; color code: green is acetonitrile, orange is dichloromethane, black is solvent-independent. The energy of the singlet MLCT/LLCT excited states has been taken as an approximate value from the maximum of the absorption spectra, the energy of the triplet MLCT/LLCT excited states has been taken for complexes **C1**, **C3**, and **C4** from the onset (5% relative intensity) of the room-temperature emission,[59] while it has been estimated for complex **C2** from the triplet MLCT/LLCT energy of **C1** plus the difference between the oxidation potentials between **C1** and **C2**, the energy of the triplet LC excited state. In **C1** and **C2**, it has been taken from the 77 K emission measurements, while the energy of the triplet LC excited state in **C3** and **C4** has to be taken as a higher-energy limit considering that phosphorescence is not observed until 850 nm (see discussion).

However, this state is still in thermal (herein slower) equilibrium with the closely lying triplet MLCT/LLCT state as disclosed by both time-resolved emission and absorption experiments (Fig. 8B). As far as complexes **C3** and **C4** are concerned, the triplet LC excited state is too low in energy with respect to the triplet MLCT/LLCT state such that mixing between these states is not feasible anymore. Consequently, the luminescence behaviour is markedly of charge-transfer character. However, the triplet LC excited state plays an important role as well in the photophysics of complexes **C3** and **C4** by enabling a non-radiative deactivation pathway to the triplet MLCT/LLCT excited state (Fig. 8C and D) and thus preventing the achievement of high emission quantum yields. Increasing the energy-gap between these two states, *e.g.*, when moving from **C3** to **C4** in acetonitrile or when changing the solvent to dichloromethane, causes indeed only slight improvements in terms of luminescence yields up to a (probably limiting) value of *ca.* 3%. As a final remark, as observed in the case of ruthenium(II) complexes with extended aromatic ligands such as those used in this work[58] and on the basis of the electrochemical data (see above), a charge transfer state involving oxidation of the iridium and reduction of the ligand in the substituted pyrazine position could be in principle populated. These states are known to be dark, non-emissive ones and to play a particularly relevant role at low temperatures.[62] Therefore, the absence of clear, spectroscopic signatures of such states definitely rules out their involvement, at least under the room temperature conditions employed herein, in the photophysics of complexes **C1–4**.

Conclusions

In this work, the synthesis of new ppl derivatives bearing methyl-pyrazole (**L1**) and thiophene (**L2**) moieties was successfully achieved. These ligands in combination with ppy and F_2-ppy cyclometalating ligands were used to obtain four new cationic Ir(III) complexes with the general formula $[Ir(R\text{-}ppy)_2(Ln)](PF_6)$. All compounds were characterized by the NMR, FT-IR, and HRMS techniques. From the HRMS and NMR data, the mononuclear nature of these complexes was confirmed. Besides, the NMR data showed an electron-donating character of the ancillary ligands evidenced by a magnetic de-shielding effect in the coordinated ligands **L1** and **L2** in comparison with their chemical shifts as free species. Importantly, **L2** has a more conjugated aromatic portion than **L1**, promoting higher chemical-shift differences between complexes **C3–4** than **C1–2**.

The photophysical behaviour of the complexes shows a clear influence depending on the substitution in both the cyclometalating and ancillary ligands. The **L1** ligand plays an important role in the nature of the emissive state of complexes **C1–2** where a complex interplay between the MLCT/LLCT and LC states has been identified by both the steady-state and time-resolved techniques. At room temperature and under fluid conditions, an apparent switch from a mixed LC/MLCT/LLCT phosphorescence in **C1** to an almost pure triplet LC luminescence in **C2** is followed. In the case of ligand **L2**, on the other hand, the appreciably low energy of the ^{3}LC excited state compared to that of the charge transfer states in the related complexes makes compounds **C3–4** practically pure charge-transfer emitters. However, the ligand-centred triplet excited state plays a non-innocent role by favouring the occurrence of non-radiative deactivation pathways that prevent the achievement of long emission lifetimes and high luminescence yields.

In summary, this work provides an additional, advanced understanding of the relationship between chemical structure and electronic properties of iridium(III) complexes for the suitable employment of such interesting compounds in diverse reasearch areas that include, among others, luminescent devices, sensors, and theranostics.

Conflicts of interest

There are no conflicts to declare.

Acknowledgements

This work was supported by FONDECYT, Chile [No. 11130221; 11160797 and 1141185]; Universidad Técnica Federico Santa María [No. 216.13.1]. I. González is grateful for a postdoctoral project, FONDECYT No. 3160285 and acknowledges the Instituto de Investigación e Innovación en Salud of Universidad Central de Chile. The authors acknowledge Dra. Sheila Lascano of Universidad Técnica Federico Santa María for the help in the experimental measurements and discussions.

References

1 S. Fantacci and F. De Angelis, *Coord. Chem. Rev.*, 2011, **255**, 2704–2726.
2 M. S. Lowry and S. Bernhard, *Chem. – Eur. J.*, 2006, **12**, 7970–7977.
3 H. J. Bolink, L. Cappelli, S. Cheylan, E. Coronado, R. D. Costa, N. Lardies, M. K. Nazeeruddin and E. Orti, *J. Mater. Chem.*, 2007, **17**, 5032–5041.
4 Q. Zhao, T. Cao, F. Li, X. Li, H. Jing, T. Yi and C. Huang, *Organometallics*, 2007, **26**, 2077–2081.
5 G. Di Marco, M. Lanza, A. Mamo, I. Stefio, C. Di Pietro, G. Romeo and S. Campagna, *Anal. Chem.*, 1998, **70**, 5019–5023.
6 X. Wang and O. Wolfbeis, *Chem. Soc. Rev.*, 2014, **43**, 3666–3761.
7 L. Flamigni, A. Barbieri, C. Sabatini, B. Ventura and F. Barigelletti, *Photochemistry and Photophysics of Coordination Compounds II*, Springer, Berlin, Heidelberg, 2007, pp. 143–203.
8 E. I. Mayo, K. Kilså, T. Tirrell, P. I. Djurovich, A. Tamayo, M. E. Thompson, N. S. Lewis and H. B. Gray, *Photochem. Photobiol. Sci.*, 2006, **5**, 871–873.
9 S. Di Bella, C. Dragonetti, M. Pizzotti, D. Roberto, F. Tessore and R. Ugo, *in Molecular Organometallic Materials for Optics*, Springer, 2010, pp. 1–55.
10 C. Dragonetti, S. Righetto, D. Roberto, A. Valore, T. Benincori, F. Sannicolò, F. De Angelis and S. Fantacci, *J. Mater. Sci.: Mater. Electron.*, 2009, **20**, 460–464.
11 K. K.-W. Lo, C.-K. Chung and N. Zhu, *Chem. – Eur. J.*, 2006, **12**, 1500–1512.

12 M. S. Lowry, J. I. Goldsmith, J. D. Slinker, R. Rohl, R. A. Pascal, G. G. Malliaras and S. Bernhard, *Chem. Mater.*, 2005, **17**, 5712–5719.
13 K. K. W. Lo, C. K. Chung and N. Zhu, *Chem. – Eur. J.*, 2006, **12**, 1500–1512.
14 M. Arias, J. Concepción, I. Crivelli, A. Delgadillo, R. Díaz, A. Francois, F. Gajardo, R. López, A. M. Leiva and B. Loeb, *Chem. Phys.*, 2006, **326**, 54–70.
15 J. R. Schoonover, W. D. Bates and T. J. Meyer, *Inorg. Chem.*, 1995, **34**, 6421–6422.
16 B. López and L. Loeb, *J. Chil. Chem. Soc.*, 2004, **49**, 83–87.
17 Y. Sun, Y. Liu and C. Turro, *J. Am. Chem. Soc.*, 2010, **132**, 5594–5595.
18 C. Chiorboli, M. A. Rodgers and F. Scandola, *J. Am. Chem. Soc.*, 2003, **125**, 483–491.
19 R. D. Costa, E. Ortí, H. J. Bolink, F. Monti, G. Accorsi and N. Armaroli, *Angew. Chem., Int. Ed.*, 2012, **51**, 8178–8211.
20 J. D. Slinker, J. Rivnay, J. S. Moskowitz, J. B. Parker, S. Bernhard, H. D. Abruña and G. G. Malliaras, *J. Mater. Chem.*, 2007, **17**, 2976–2988.
21 C. Ulbricht, B. Beyer, C. Friebe, A. Winter and U. S. Schubert, *Adv. Mater.*, 2009, **21**, 4418–4441.
22 S. Lamansky, P. Djurovich, D. Murphy, F. Abdel-Razzaq, R. Kwong, I. Tsyba, M. Bortz, B. Mui, R. Bau and M. E. Thompson, *Inorg. Chem.*, 2001, **40**, 1704–1711.
23 I. González, P. Dreyse, D. Cortés-Arriagada, M. Sundararajan, C. Morgado, I. Brito, C. Roldán-Carmona, H. J. Bolink and B. Loeb, *Dalton Trans.*, 2015, **44**, 14771–14781.
24 D. Cortés-Arriagada, L. Sanhueza, I. González, P. Dreyse and A. Toro-Labbé, *Phys. Chem. Chem. Phys.*, 2016, **18**, 726–734.
25 I. González, D. Cortés-Arriagada, P. Dreyse, L. Sanhueza-Vega, I. Ledoux-Rak, D. Andrade, I. Brito, A. Toro-Labbé, M. Soto-Arriaza, S. Caramori and B. Loeb, *Eur. J. Inorg. Chem.*, 2015, 4946–4955.
26 G. F. Strouse, J. R. Schoonover, R. Duesing, S. Boyde, W. E. J. Jones and T. J. Meyer, *Inorg. Chem.*, 1995, **34**, 473–487.
27 R. Horvath and K. C. Gordon, *Inorg. Chim. Acta*, 2011, **374**, 10–18.
28 A. Francois, R. Díaz, A. Ramírez, B. Loeb, M. Barrera and I. Crivelli, *Polyhedron*, 2013, **52**, 62–71.
29 A. E. Friedman, J. C. Chambron, J. P. Sauvage, N. J. Turro and J. K. Barton, *J. Am. Chem. Soc.*, 1990, **112**, 4960–4962.
30 L. Hu, Z. Bian, H. Li, S. Han, Y. Yuan, L. Gao and G. Xu, *Anal. Chem.*, 2009, **81**, 9807–9811.
31 F. Shao, B. Elias, W. Lu and J. K. Barton, *Inorg. Chem.*, 2007, **46**, 10187–10199.
32 G. Čík, J. Krajčovič, P. Veis, D. Végh and F. Šeršeň, *Synth. Met.*, 2001, **118**, 111–119.
33 J. P. Nietfeld, R. L. Schwiderski, T. P. Gonnella and S. C. Rasmussen, *J. Org. Chem.*, 2011, **76**, 6383–6388.
34 C. B. Larsen, H. van der Salm, C. A. Clark, A. B. Elliott, M. G. Fraser, R. Horvath, N. T. Lucas, X.-Z. Sun, M. W. George and K. C. Gordon, *Inorg. Chem.*, 2014, **53**, 1339–1354.
35 T. Sajoto, P. I. Djurovich, A. B. Tamayo, J. Oxgaard, W. A. Goddard III and M. E. Thompson, *J. Am. Chem. Soc.*, 2009, **131**, 9813–9822.
36 S. Salinas, M. Soto-Arriaza and B. Loeb, *Polyhedron*, 2011, **30**, 2863–2869.
37 K. K.-W. Lo, J. S.-W. Chan, L.-H. Lui and C.-K. Chung, *Organometallics*, 2004, **23**, 3108–3116.
38 K. Butsch, R. Gust, A. Klein, I. Ott and M. Romanski, *Dalton Trans.*, 2010, **39**, 4331–4340.
39 P. Dreyse, I. González, D. Cortés-Arriagada, O. Ramírez, I. Salas, A. González, A. Toro-Labbe and B. Loeb, *New J. Chem.*, 2016, **40**, 6253–6263.
40 M. K. Kuimova, W. Z. Alsindi, A. J. Blake, E. S. Davies, D. J. Lampus, P. Matousek, J. McMaster, A. W. Parker, M. Towrie and X.-Z. Sun, *Inorg. Chem.*, 2008, **47**, 9857–9869.
41 M. G. Fraser, A. G. Blackman, G. I. Irwin, C. P. Easton and K. C. Gordon, *Inorg. Chem.*, 2010, **49**, 5180–5189.
42 Y. You and S. Y. Park, *J. Am. Chem. Soc.*, 2005, **127**, 12438–12439.
43 A. Beeby, S. Bettington, I. D. Samuel and Z. Wang, *J. Mater. Chem.*, 2003, **13**, 80–83.
44 C. Zúñiga, I. Crivelli and B. Loeb, *Polyhedron*, 2015, **85**, 511–518.
45 L. Wang, W. Qin and W. Liu, *Inorg. Chem. Commun.*, 2010, **13**, 1122–1125.
46 S. Reineke and M. A. Baldo, *Sci. Rep.*, 2014, **4**, 3797.
47 C. Cebrián, M. Natali, D. Villa, M. Panigati, M. Mauro, G. D'Alfonso and L. De Cola, *Nanoscale*, 2015, **7**, 12000–12009.
48 A. P. Wilde, K. A. King and R. J. Watts, *J. Phys. Chem.*, 1991, **95**, 629–634.
49 M. Schmittel and H. Lin, *Inorg. Chem.*, 2007, **46**, 9139–9145.
50 Y. You and W. Nam, *Chem. Soc. Rev.*, 2012, **41**, 7061–7084.
51 L. Troian-Gautier and C. Moucheron, *Molecules*, 2014, **19**, 5028–5087.
52 X. Li, B. Minaev, H. Ågren and H. Tian, *Eur. J. Inorg. Chem.*, 2011, 2517–2524.
53 S.-C. Lo, C. P. Shipley, R. N. Bera, R. E. Harding, A. R. Cowley, P. L. Burn and I. D. Samuel, *Chem. Mater.*, 2006, **18**, 5119–5129.
54 E. Orselli, R. Q. Albuquerque, P. M. Fransen, R. Fröhlich, H. M. Janssen and L. De Cola, *J. Mater. Chem.*, 2008, **18**, 4579–4590.
55 C.-H. Yang, J. Beltran, V. Lemaur, J. Cornil, D. Hartmann, W. Sarfert, R. Fröhlich, C. Bizzarri and L. De Cola, *Inorg. Chem.*, 2010, **49**, 9891–9901.
56 S. Lamansky, P. Djurovich, D. Murphy, F. Abdel-Razzaq, H.-E. Lee, C. Adachi, P. E. Burrows, S. R. Forrest and M. E. Thompson, *J. Am. Chem. Soc.*, 2001, **123**, 4304–4312.
57 P.-T. Chou, Y.-I. Liu, H.-W. Liu and W.-S. Yu, *J. Am. Chem. Soc.*, 2001, **123**, 12119–12120.
58 J. Seo, S. Kim and S. Y. Park, *J. Am. Chem. Soc.*, 2004, **126**, 11154–11155.
59 M. Indelli, M. Ghirotti, A. Prodi, C. Chiorboli, F. Scandola, N. McClenaghan, F. Puntoriero and S. Campagna, *Inorg. Chem.*, 2003, **42**, 5489–5497.
60 K. Y. Lu, H. H. Chou, C. H. Hsieh, Y. H. O. Yang, H. R. Tsai, H. Y. Tsai, L. C. Hsu, C. Y. Chen, I. Chen and C. H. Cheng, *Adv. Mater.*, 2011, **23**, 4933–4937.
61 F. Lafolet, S. Welter, Z. Popović and L. De Cola, *J. Mater. Chem.*, 2005, **15**, 2820–2828.
62 M. K. Brennaman, T. J. Meyer and J. M. Papanikolas, *J. Phys. Chem. A*, 2004, **108**, 9938–9944.

